THE AMERICAN MINERALOGIST, VOL. 48, JULY-AUGUST, 1963

PHASE TRANSFORMATION AND THERMAL HYSTERESIS IN THE SYSTEM AgI

CECIL J. SCHNEER AND RICHARD W. WHITING, JR.,
Dept. of Geology and Geography and Dept. of Chemical Engineering, University of New Hampshire, Durham, N. H.

ABSTRACT

A process of thermal diffraction analysis (TDA) yields direct curves of p *vs* T; p is the proportion of α-AgI. Mixtures of the γ- and β-AgI phases transform heterogeneously to α-AgI according to the empirically derived equations, $p/(1-p)=\exp.\ (-\Delta f/kT)$; and $-\Delta f=Q-Ts$; Δf is the difference in energy between particles in the high and low states at the temperature T; Q and s are constants; $Q=3.63\times10^5$ cal/mol, $s^{low\text{-}high}$ (423° K) = 858 cal/mol-deg; and $s^{high\text{-}low}$ (411° K.) = 883 cal/mol-deg. The transformation is anisothermal because there is a mixing reduction in the free energy. Hysteresis is attributed to friction. The hysteresis loss is *ca.* 250 cal/mol. Ordinarily, low AgI is a $\beta+\gamma$ mixture, the proportion of γ being measured by a parameter D which is a function of the relative diffraction intensities. Little isothermal transformation between β and γ is observed, but samples transforming from the high α phase are about D(.40), regardless of the initial value of D of the sample. The hysteresis loss is slightly less for samples which were initially high D and this persistence of the influence of the previous state through transformation is attributed to a disordering within the α phase, influenced by the parameter D.

INTRODUCTION

The phase transformations of AgI are of significance because of the structural analogy with zinc sulfide, silicon carbide, cadmium sulfide, manganese sulfide and other AX compounds crystallizing with the B4 and B3 structures. The three principal phases of AgI are the γ or B3 or sphalerite-type low temperature cubic polymorph (miersite) (*Strukturberichte* **I,** 1913–1926; **III,** 1933–1935); the β or B4 or wurtzite-type temperature hexagonal polymorph (iodyrite) (*Strukturberichte* III; 1933–1935); and the α or (B23) high temperature polymorph, having a body-centered cubic structure of iodine with silver atoms randomly distributed through the interstices (Strock, 1936). Exceptionally high ionic conductivity for this form at 146° C. is interpreted to indicate free diffusion or a quasi-fluid state of the silver within the iodine framework. A fourth high pressure form with the NaCl structure has been described (*Strukturberichte* **VI,** 1938). Polytypism within the low temperature $\gamma+\beta$ system may have been observed and has been suggested.

The low temperature $\gamma+\beta$ system will be referred to below as close-packed because the iodine atoms are in the same patterns as those for the close packing of spheres. The numerous references to AgI are in essential agreement on a transformation from the close-packed form to the α form above about 146° C. This transformation exhibits hysteresis, occurring at temperatures 12° apart for the appearance and disappearance of the α phase.

The transformation between the two close-packed forms γ and β is reported to occur between 125 and 135° C. (Bloch and Möller, 1931) but the TDA curves shown below and the numerous trials made of which these curves are representative, fail to show a critical transition temperature in this range or indeed in any range from the α-transformation temperature down to dry ice temperatures. Theoretical studies (Schneer, 1955) suggest that the transformation from a cubic close packed form to a hexagonal close packed form should not proceed at a single temperature but that mixtures of the two close packed phases are in equilibrium at all temperatures below a critical temperature, the proportion of the hexagonal close packed phase to the cubic close packed phase increasing with temperature in a manner mathematically analogous to the increase of disorder in a metal.

In order to study the thermal dependence of the transformations and to examine the hysteresis in detail, a process of continuous x-ray diffraction which we call thermal diffraction analysis (TDA), was employed. This showed that the transformation between close packed phases (γ to β or β to γ) was essentially athermal, that is, independent of temperature—a result confirmed by prolonged heat treatment trials. Since this transformation is theoretically one of degree, the quantitative analysis of the x-ray diffractogram was critical. Procedures were developed for the synthesis of γ and β—AgI with diffraction patterns in substantial agreement with computed patterns. We are using the term *thermal diffraction analysis* (TDA) to mean the diffraction of x-rays by a sample undergoing heating or cooling at definite rates. There are well established x-ray procedures for the study of phase transformation by obtaining diffraction patterns of samples at temperatures which are fixed. Interpolation between these fixed temperatures indicates the kind and degree of structural change that has occurred during the heat treatment of these samples, but this is development which has occurred and is complete at the time of analysis. The development of the diffractometer makes it possible to study the kind and degree of structural change occurring during the heat treatment of samples. In other words, the change is analyzed while it is occurring. One procedure described as continuous x-ray diffraction (Wahl *et al.* 1961) is to use the x-ray diffractometer to scan back and forth over a small angle $\Delta 2\theta$, while continuously raising the temperature of the sample. The peak heights of key lines are then plotted as a function of temperature (Fig. 6). It is also possible, if care is taken to remain on the peaks, to obtain continuous records of peak height *vs.* time on a strip chart recorder, while the temperature is being raised or lowered at a constant rate. From the two records of intensity *vs.* time and temperature *vs.* time, graphs of intensity *vs.* temperature may be constructed. Since the absorption of x-rays by high and low temperature phases is nearly equal,

the intensity of a diffraction peak is close to a linear function of the proportion of the phase containing the inter-planar spacing responsible for the peak. A third and by far the most satisfactory procedure is to plot peak intensity *vs.* temperature directly on an X-Y recorder (see below).

From the curves of the proportion of the phase against temperature, we are able to derive empirical equations of proportion of phase as a function of temperature, which are cast in the form of the Boltzmann equation. Identifying the constants in the empirical equation with parallel terms for the Boltzmann equation, the curves make possible the evaluation of a series of thermochemical coordinates and a detailed examination of the process of phase transformation.

Thermal Diffraction Analysis

Figure 1 shows the diffractometer traces of the three principal AgI modifications, CuKα radiation, Ni filter, 2θ from 20 to 60 degrees. Integrated intensities by count were found to be approximately proportional to peak heights.

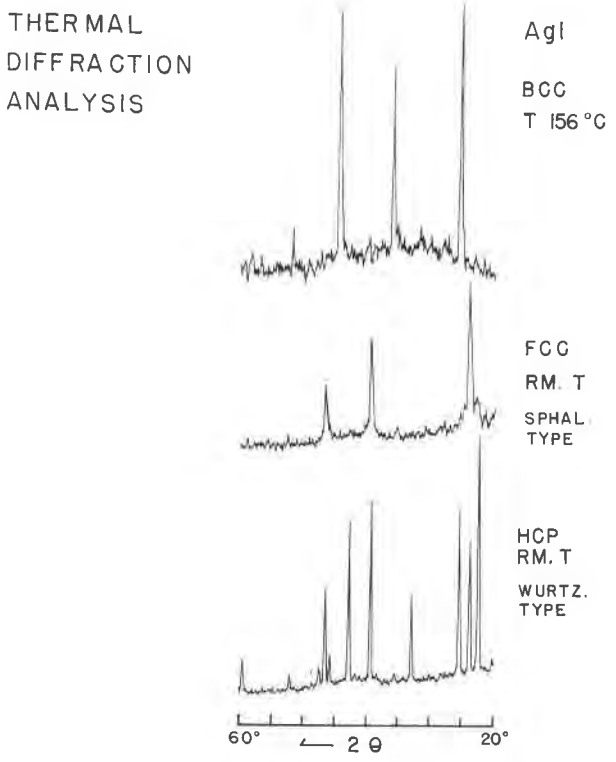

Fig. 1. Diffractometer traces 2θ 20–60° of the three principle phases of AgI, the α or BCC (B23), the γ or FCC (B3), and the β or HCP (B4); CuKα, Ni filter.

TABLE 1. PUBLISHED INTENSITIES (SWANSON ET AL., 1959) THE 12 DIFFRACTION PEAKS BETWEEN 20 AND 60° 2θ FOR β-AgI

hkl	Dow Chemical	Wilsey	N.B.S.
	MoKα	1923 MoKα	1958 CuKα
100	75	70	61
002	62	70	100
100	62	30	38
102	25	20	16
110	100	100	83
103	62	60	31
200	—	—	6
112	50	80	51
201	10	—	5
202	7	—	7
203	17	20	5
210	5	—	4

U.N.H. INTENSITIES
CuKα
COMPUTATION FOR ASSUMED PROPORTION OF β-AgI IN A $\gamma+\beta$ MIXTURE

hkl	Observed	Computed	Observed	Computed
	99.6% Hex		94.5% Hex	
100	100	100	100	100
002	58.57	58.18	66.44	67.15
101	62.08	62.86	64.49	63.63
102	32.21	34.38	37.20	34.62
110	67.27	71.02	73.88	71.28
103	65.58	63.67	58.27	58.52
200	11.12	10.39	8.22	9.94
112	41.56	38.87	39.05	38.74
201	11.61	8.41	10.43	8.91
202	4.23	6.69	5.73	7.07
203	13.92	16.81	14.88	14.48
210	4.68	5.89	4.81	5.69

All U.N.H. intensities above recalculated as per cent of strongest line for comparison with published intensities.

The three prominent lines of the cubic close-packed form are, in order of ascending 2θ, the (111), (220), and (311) characteristic of the diamond structure. These coincide in position with the (002), (110) and (112) respectively, of the hexagonal close-packed form. Intensities for the first 12 lines of the hexagonal close-packed form are given in Table 1 along with

intensities reported from the literature. The lines shown for the body-centered cubic form are the (110), (200), (211), (220), and (310) in order of ascending 2θ.

Figure 2 is a diagrammatic representation of the results of thermal diffraction analysis. To the right is the trace of 20 to 60 degrees 2θ for the starting material,—reagent AgI, obtained from Matheson, Coleman &

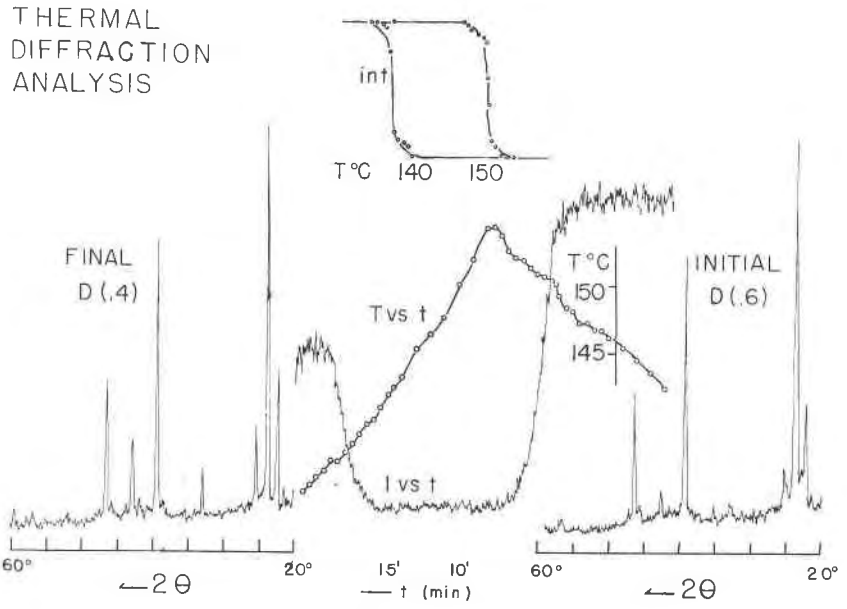

FIG. 2. The diffractogram at the right is of reagent AgI at the start of the run; the diffractogram at the left is of the same sample at the end of the run. Between the two is the curve of Intensity (002) *vs.* time in minutes running from right to left. Superimposed on the I *vs.* t curve is the curve of temperature *vs.* time. Above is the *temperature vs. proportionate intensity* loop constructed from the curves below, showing hysteresis.

Bell, CB 677, Lot #301370. The pattern is essentially the same as that obtained in other lots of commercially available AgI powder.

DETERMINATION OF THE PROPORTION OF γ TO β

The method is essentially that for the determination of phase proportions of austenite-martensite described in Cullity (1956, p. 392). The intensity of a given line is assumed equal to the computed intensity of the line for the hexagonal crystal times the fraction of the sample in the hexagonal phase plus the computed intensity of the line for the cubic crystal times the fraction of the sample in the cubic phase. Let D be an order parameter defined as giving the probability that a given unit of the sample is cubic.

$$D = \frac{n_\gamma}{n_\beta + n_\gamma}; \tag{1}$$

n_γ is the number of units which are cubic;

n_β is the number of units which are hexagonal.

$(1-D)$ is therefore the hexagonal fraction of the sample. The volume of the cubic unit cell is four times the volume of the hexagonal unit cell. The intensity of a given diffraction line is therefore proportional to

$$(1 - D)\cdot I_c(hkl) + D\cdot I_c(hkl)'\tfrac{1}{4}; \tag{2}$$

$I_c(hkl)$ is the computed intensity at a specified angle 2θ, for hexagonal β-AgI; $I_c(hkl)'$ is the computed intensity at the same angle 2θ, for cubic γ-AgI. For comparison, all intensities computed and observed are normalized by dividing the absolute intensities (computed) and integrated intensities (observed) by the sum (s_1) of the absolute intensities (computed) or integrated intensities (observed) of the first four hexagonal lines.

$$s_1 = \sum \text{Int.}\,[(100), (101), (102), (103)] \tag{3}$$

While in theory the order parameter D could be obtained from the diffraction intensity at a single angle, error is reduced by considering a ratio (r) of the sum of the observed intensities of the first four hexagonal lines to the sum of the observed intensities of the first three prominent lines common to both the cubic and hexagonal diffraction patterns.

$$r_{obs.} = \frac{s_1}{\sum \text{Int.}\,[(002), (110), (112)]}; \tag{4}$$

All intensities are referred to hexagonal indices.

There are only two lines, in the interval $2\theta < 60°$, the cubic (200) and (400), which are not common to the hexagonal phase. Since these are weak, they were not chosen as index lines.

Referring to (2), r may be computed as a function of D:

$$r_{calc.} = \frac{s_1}{(1 - D)\cdot s_2 + D\cdot s_3/4}; \tag{5}$$

s_2 is the sum of the computed hexagonal intensities (002), (110), and (112); s_3 is the sum of the computed intensities of cubic AgI at the same angles 2θ, with cubic Miller indices (111), (220) and (311). Figure 3 is the graph of $r_{calc.}$ *vs.* $1-D$. The complete curve is for an average temperature factor $\bar{u}$ (.25) Å. Note that all intensities in (4) are observed; all intensities in (5) are computed. Since the determination of D rests on the computation of intensities for (5), the value of D in general will be sensitive to all parameters entering into the equation for intensity calculations, such as: a) and b) the separate temperature factors, c) their anisotropy, d) the unit cell coordinates, e) preferred orientation of grains in the diffractome-

ter sample, etc. Partial curves of Fig. 3 are for lower values of ū. Reasonably consistent values of D may be obtained directly from the graph, using peak heights for observed intensities, while more precise values of D are computed from integrated intensities, taking a, b, c, d and e into account.

The reagent AgI with diffractogram shown in Fig. 2 (initial) was approximately 60% cubic, D(0.6). With the diffractometer fixed on the (002) trace, the temperature was increased as shown on the temperature *vs.* time graph (Fig. 2, center). The transformation as shown by the disappearance of the (002) line, occurred with intensity falling off as an s-shaped function of time. On reversing the direction of the temperature change the s-shaped reappearance of the (002) spacing occurs at a tem-

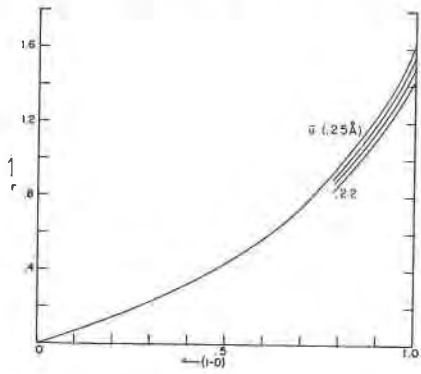

FIG. 3. r *vs* (1−D). The ratio of the sum of the relative integrated intensities of the first four diffraction lines found only in the β-AgI record, (100, 101, 102, 103) to the sum of the relative integrated intensities of the three major lines common to β and γ patterns, (002, 110, 112) in hexagonal indices) plotted as a function of D, the proportion of γ-phase present. The upper curve is for an average thermal displacement (ū) of the atoms from their ideal positions, of .25 Å. The lower three partial curves illustrate the effects of assumed ū values of .24, .23, and .22 Å.

perature below the temperature of the transformation on the initial part of the run. The diffractometer trace to the left is of the same sample cooled back to room temperature. The proportion of cubic to hexagonal has declined from D(0.6) to approximately D(0.4). Thermal hysteresis is shown in the small graph of the proportion of close-packed AgI *vs.* temperature (Fig. 2, top, center).

Figure 4 is a similar composite diagram made from the traces of AgI before and after carrying the sample around the hysteresis loop (shown with the diffractometer trace of (002) intensity *vs.* time, in the center of the diagram). The starting material was approximately D(0.97). The final material was approximately D(0.40) as before. Figure 5 illustrates the same procedure with initial material all hexagonal D(0.0) and final material again D(0.40). We believe that these results are reproducible and that regardless of the value of the parameter D in the starting material, we approach D (0.40) on emerging from the loop. But in some instances, D(0.0) material remained substantially hexagonal (D(0.1−0.2))

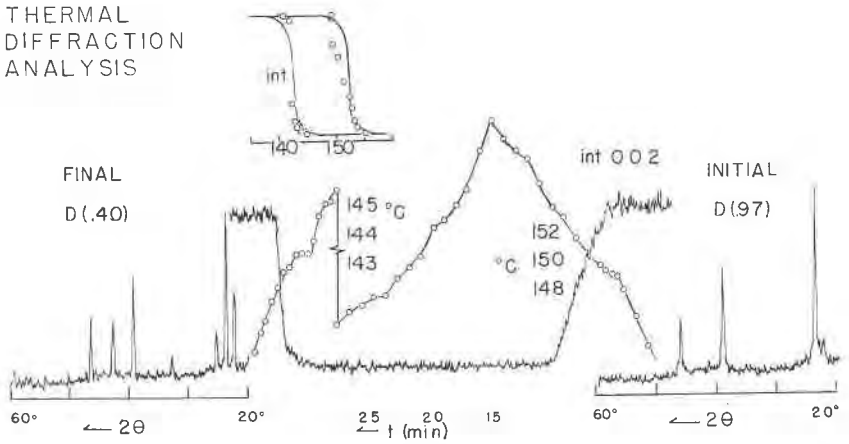

FIG. 4. As in Fig. 2, diffractograms before (right) and after (left) TDA, with *Intensity* (002) and *Temperature vs. time* curves and the hysteresis loop of *proportionate intensity vs. temperature*. The starting material is 96% γ-or FCC (B3) AgI. Note the appearance of the 100, 101, 102 and 103 diffraction lines in the final pattern.

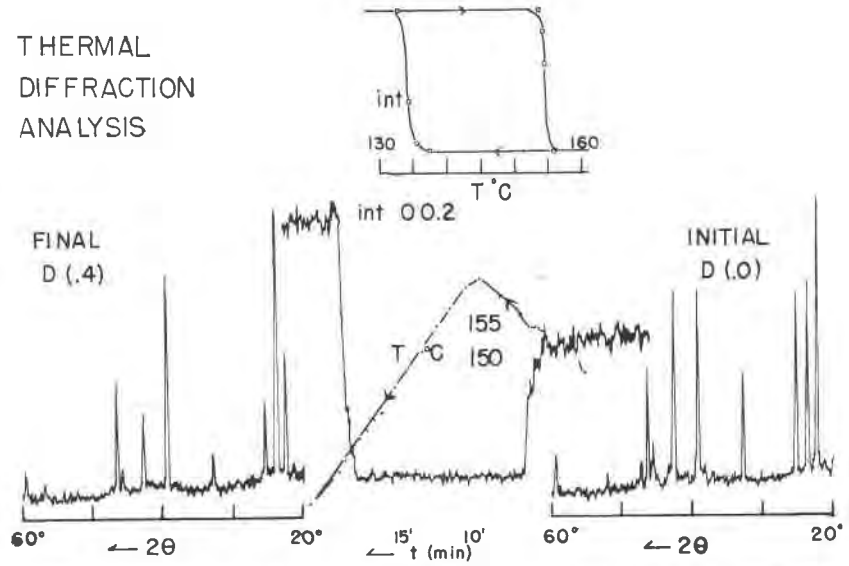

FIG. 5. As in Figs. 2 and 4 but with starting material nearly 100% β or HCP (B4) AgI. Compare initial diffractogram (right) with type diagram for β of Fig. 1. The final diffractogram (left) is comparable to the final diffractograms (left) in Figs. 2 and 4. The proportion of γ-phase after the transformation approaches 40% regardless of the proportion before the transformation. But the hysteresis loop is widest for samples initially low in γ.

after holding it for one hour in the α form at 146° C. and then reconverting to the low temperature form. Repeating the cycle brings such material to D(0.4).

We also attempted to converge on this final value of D by holding samples at constant temperatures below the transformation temperature. If D(0.40) is the equilibrium ratio characteristic of a temperature of about 143° C., all samples with other values of D should change at this temperature. Cubic samples transform isothermally towards the D(0.40) value but hexagonal samples (low D) did not change appreciably. In dynamic runs (Fig. 6) the emergence of distinct hexagonal (100) and (101) lines from almost the background level of an initially high D (cubic) sample contrasts with the slight falling off of the ratio of intensities of the hexagonal (100) to the common (002) line for an initially D(0.0) (hexagonal) sample. It would appear that the transformation of the hexagonal close-packed to the cubic close-packed structure is not readily accomplished isothermally. We were in fact unable to accomplish this transformation to any considerable degree by various heat treatments including quenching to dry ice temperatures. Transformation to D(0.97) approximately, was accomplished by repeated grinding with temperature falling from 100° C. to room temperature. The absence of an appreciable rate of isothermal transformation does not prove anything about equilibrium but indicates that the transformation is either diffusionless (the so-called martensitic type of phase transformation) or relatively diffusionless.[1]

In order to establish the reality of the hysteresis loop, a series of runs were made in the attempt to explore the interior of the loop. The temperature was increased (run 3, Fig. 7) until the transformation was observed to begin on the continuous record of the intensity of the (002) line. The temperature was then abruptly reversed before the (002) line had disappeared. Within the loop with the temperature held steady, it was possible to obtain a complete diffractometer record for the 20 to 60 degree 2θ range. The low temperature $\beta+\gamma$ close-packed pattern was superposed on the high temperature α phase pattern. Although this transition is described as a rapid, "first-order," reaction, it was possible after $6\frac{1}{2}$ hours within the loop to obtain both patterns superimposed. On other trials (run 7a) it proved possible to enter the loop by cooling down the high temperature phase and heating when the transformation began. It ap-

[1] The formation of martensite, a body-centered tetragonal iron with minor entrapped carbon, is athermal (occurs with changing temperature) and is therefore attributed to shear rather than to diffusion. The transformation is time-independent with the fraction transformed at a given temperature a function of the temperature rather than of the time taken to reach the temperature or held at the temperature (see below).

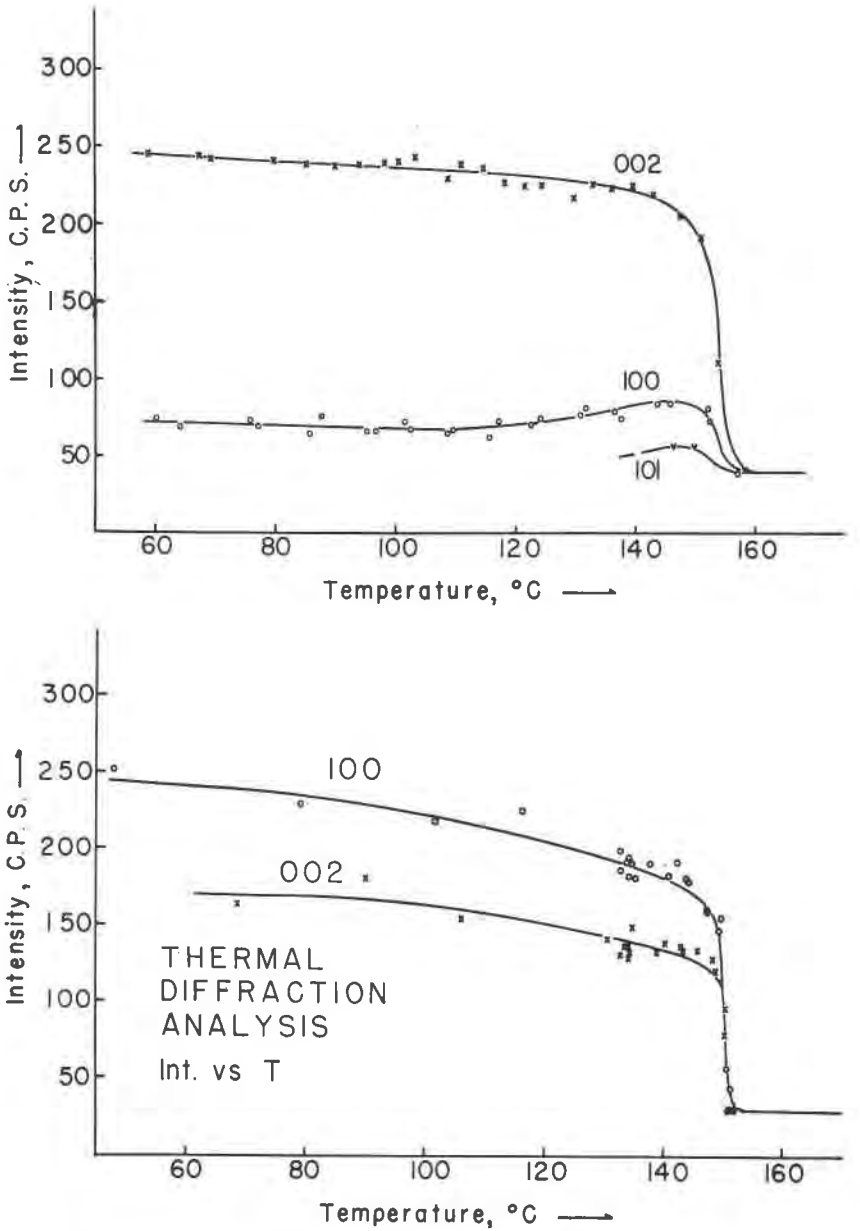

FIG. 6. Continuous x-ray diffraction. Peak intensities of critical lines are plotted as a function of temperature. In the upper graph, the starting material was (largely) γ-AgI; in the lower graph, the starting material was β-AgI. Note that the reported γ to β transformation at 125–135° C. was not observed, either in these or other runs.

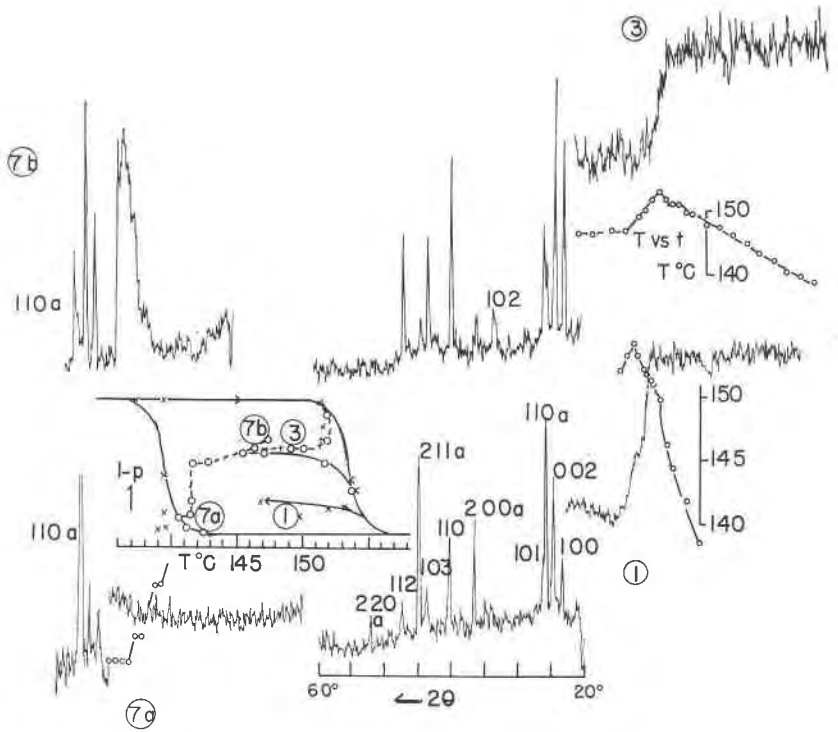

FIG. 7. Interior of the hysteresis loop. The hysteresis loop is plotted as the proportion of *low temperature* AgI (1-p) *vs. temperature*. The first run marked with crosses, began at the upper left corner of the loop and entered the loop in a cw sense. The trace of the (100) line is shown in the lower right diagram with *temperature vs. time* superposed. Time ran from right to left at the rate of five minutes per inch, or ½ minute per chart division. The third run marked with circles also enters the loop in a cw sense. Intensity (100) and *temperature vs. time* graphs are reproduced upper right, above the same graphs for run 1. Complete scans from 20 to 60° 2θ are reproduced in the center of the diagram. The traces for run 1 in the lower scan are indexed with hkl_α distinguishing the indices for the α-phase. With scanning rate 2° per minute, both scans represent 20 minute intervals, during which the specimens were at positions within the loop represented respectively by the last cross of the line marked 1, and the last circle of the line marked 3. Run 3 is shown leaving the loop in a cw sense. Plus signs represent a duplication of the first part of run 3. Circles are used to show run 7 entering the loop from below with the initial increase in intensity (100) shown lower left and a partial diffractometer scan to show the prominent (110_α) at the position marked 7a. Further increase in proportion of the low temperature phases $\gamma+\beta$ is shown in the graph 7b upper left by the abrupt rise in intensity (100) with the partial diffractometer scan showing the decline in the intensity of the (110_α).

pears possible to arrive at any point within the loop and to remain at that point indefinitely. At any temperature within the band of temperatures embracing the loop, any proportion of high to low-temperature phase

may be obtained. These phenomena parallel the familiar hysteresis associated with ferromagnetism and ferroelectricity. Extensive thermal hysteresis has been reported in metallurgical literature (Kaufman and Cohen, 1958).

The hysteresis loops of Figs. 2, 4 and 5, top center, appear to indicate that the width of the loop is inversely proportional to the D of the starting material. Bloch and Möller (1931) reported that the proportion, D, of the starting material, was again obtained after cycling through the transformation, *i.e.* that AgI after undergoing the transformation to α (accompanied by a marked decrease in volume) is, upon transforming back, influenced by its earlier state of aggregation. While we were unable to obtain this persistence of the parameter D consistently, and in fact obtained D(0.4) (approximately) in most runs, the width of the loop did appear to be related to the initial value of D. Narrowing of hysteresis loops by plastic deformation is well known for martensitic transformations (Kaufman and Cohen, 1958). Presumably, deformation stimulates nucleation of the stable phase when simple heating or cooling may be insufficient. On this basis, since our γ-AgI was made from β-AgI by grinding, we might account for a lowering of the temperatures for the upper end of our loop, but no deformation of the high AgI was performed, and therefore, the apparent memory or persistence of the influence of the earlier state of aggregation through the transformation cycle is not explained by previous grinding.

We believe that this memory can be explained by the hypothesis that the degree of disorder in the α phase is determined by the degree of disorder of the initial material. By considering the cubic-hexagonal close-packing transition on a layer for layer basis, D can be considered an order parameter with $1-D$ measuring the proportion of stacking faults (Schneer, 1955). Then let D′ be an order parameter for the α phase. The persistence of an influence of D through a complete cycle from $\beta+\gamma$ to α and back to $\beta+\gamma$ might be explained by the assumption that D′ (and the final D) depend upon the initial D to a degree depending upon the history of the sample treatment in this range. Such a persistence of order through bcc to cp phase transformation was suggested in 1939 by Greninger for β-CuAl alloys.

Shape of the Hysteresis Loop

Figure 2 illustrates the shape of the intensity *vs.* time curve. When AgI transforms with either rising or falling temperature, the transformation begins slowly and proceeds more and more rapidly (first part of the s-curve). The greatest part of the transformation or the greatest rate of transformation occurs at the central, almost vertical part of the s-curve

Finally the rate of transformation declines, intensity approaching a constant level asymptotically. Instrumental difficulties not yet completely overcome introduce irregularities and ambiguities in the curves but a careful study of more than twenty-five full cycles suggests that the ƨ-curve is accurate to at least a first approximation. Inverse, or s-curves are obtained when the diffractometer is set at the angle for the (110) line of the high temperature α phase. The temperature *vs.* time curves of Figs. 2, 4 and 5 center superposed on the diffractometer traces, suggest but do not clearly indicate platforms. These curves were obtained from potentiometer readings which we attempted to make at half-minute intervals in critical parts of the process.

The intensity *vs.* temperature curves making up the hysteresis loops in Figs. 2, 4 and 5 and in almost all of at least 25 separate cycles, are of this tripartite, s or ƨ character. We have observed the transformation taking place by lifting the cover of the *x*-ray heating stage. The α phase is a bright orange yellow, the $\beta+\gamma$ mixture is a pale yellow. The β phase is a dull yellow and the γ is a brighter lemon yellow. As the flat sample of α-AgI powder cools through the transformation, a sprinkling of yellow dots appears on the orange surface. The yellow spots expand rapidly, coalescing until the pattern is one of spotty orange remnants on a yellow field. These in turn disappear, the entire process proceeding to completion under air cooling in about two minutes. (It has not been established that the color changes *necessarily* coincide with the phase changes.) Pitzer (1941) believes that there is a shift towards red with increasing temperature.

Figure 8 shows hysteresis loops traced directly and continuously on a X-Y Recorder with ordinate axis connected in parallel to the diffractometer recorder and abscissa axis connected through a DC amplifier to a thermocouple in contact with the platinum sample holder. No part of the transformation is isothermal. Decreasing the rate of heat transfer serves to smooth the s-curves, but not to straighten them. The transformation is distinctly anisothermal.

The AgI Thermal Diffraction Curves

Let p and $1-p$ represent respectively the probability that a particle is in the high and low temperature phases. Using values from the thermal diffraction curves of Fig. 8a, the graph (Fig. 9) of $1/T$ *vs.* $\ln p/(1-p)$ is a straight line. In slope-intercept form,

$$1/T = m \ln \frac{p}{1-p} + b. \tag{6}$$

m is the slope and *b*, the intercept, for the line of Fig. 9.

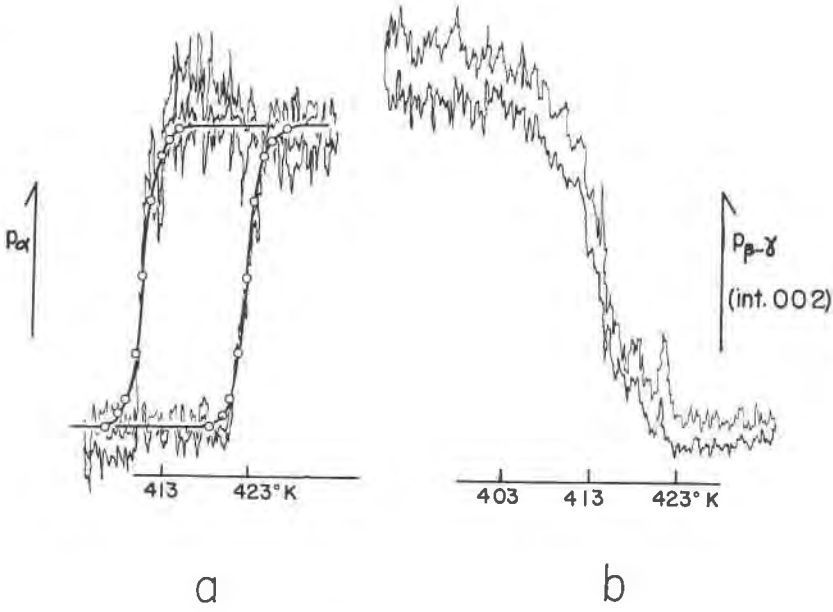

FIG. 8. Thermal diffraction analysis. Continuous record of intensity *vs.* temperature.
a. P_α *vs.* T

P_α is the proportion of the α-phase measured as the intensity of the (110_α); a tracing from the X-Y recorder sheet. The constructed curves and points are the source of the figures used for the computations of the empirical equations.

b. $P_{\beta+\gamma}$ *vs.* T

$P_{\beta+\gamma}$ is measured as proportion of intensity of (002). The sample was doped with traces of Cu. This is a tracing of the X-Y recorder sheet with Y axis driven by the *x*-ray ratemeter circuit and *X* axis by the amplified signal from a Pt-Rh thermocouple in contact with the Pt sample holder.

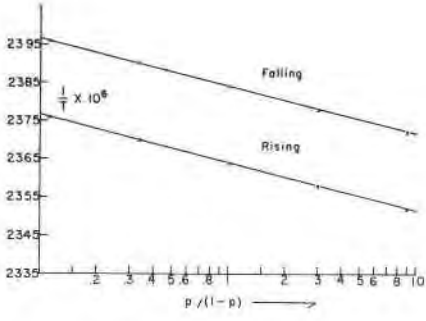

FIG. 9. 1/T *vs.* ln n p/(1−p). p and (1−p) are the probabilities that a particle is in the high and low temperature phases, respectively. Values are taken from Fig. 8a with the upper line for the transformation with falling and the lower line for the transformation with rising temperature.

Then, introducing a series of constants, k, Q and s; such that k is the Boltzmann constant;

$$Q = \frac{k}{m}, \qquad \text{(since m is a constant);} \tag{7a}$$

and $$s = bQ, \qquad \text{(since b is a constant);} \tag{7b}$$

then from (6) and (7), $$\frac{p}{1-p} = e^{(Q-Ts)/kT}; \tag{8}$$

Let $-\Delta f$ represent the function $(Q-Ts)$;

$$-\Delta f = Q - Ts, \text{ plotted as Fig. 10.} \tag{9}$$

$$\frac{\partial \Delta f}{\partial T} = s = \text{constant.} \tag{10}$$

That is, the results of TDA have been cast in the form of the Boltzmann equation indicating the statistical distribution of the two phases according to an energy term (Q-Ts). The proportionate distribution of the particles between the high and low temperature phases, $p/(1-p)$ as a function of temperature was obtained by TDA. Then the difference in energy between particles in the two phases is derived as a function of T in (9) and shown to be linear in (10).

The constant Q governs the slope of the graph (9). For very large Q, the $1/T$ *vs.* $\ln p/1-p$ lines are horizontal and the transformation is isothermal. The departure of the TDA curves from the isothermal is inversely proportional to Q. At the median temperature T_m, $p=1-p=0.5$ and $\ln p/(1-p)=0=-\Delta f$. Therefore from the TDA curves of 8a,

$$Q^{L-H} = Q^{H-L} = 3.63 \times 10^5 \text{ cal/mol.} \tag{11}$$

The constant s determines T_m; the larger the value of s, the lower the, temperature of transformation. From the observed values of T_m; $T_m{}^{L-H}$ (423), $T_m{}^{H-L}$ (411)°K.;

$$s^{L-H} = 8.58 \times 10^2 \text{ cal/mol-deg;} \tag{12a}$$

$$s^{H-L} = 8.83 \times 10^2 \text{ cal/mol-deg;} \tag{12b}$$

In 1938 Becker obtained equations similar to (8) and (9) for the ordering transformation in the system Au-Pt. He designated Δf as the energy for the formation of a stable nucleus at the temperature T, and Q as the activation energy for diffusion.

Our transformation is apparently diffusionless. This is established by the series of runs summarized in Fig. 7 which demonstrates that to a first approximation, the transformation is time-independent. We therefore interpret Q as the formal activation energy for the formation of a stable nucleus at the absolute 0. Δf decreases linearly with temperature (Eq. 10,

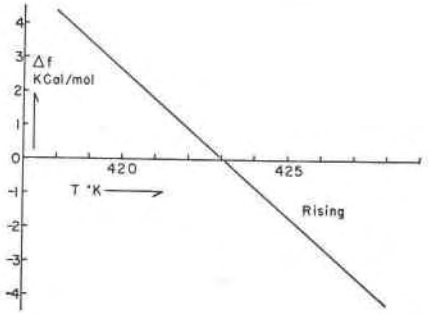

FIG. 10. Δf *vs.* T for transformation with rising temperature.

Fig. 10) until at 418° K with the value 4.36 Kcal/mol, a few nuclei of the high temperature phase are stable. Near 423° K, the probability that a given crystallite is in one or the other level, is equal. Beyond 423° K, the driving term, $-\Delta f$, decreases until at 428° K, the probability of a given crystallite remaining in the lower phase is negligible.

From the curves of Fig. 8a, we obtain:

$$p = g(\Delta f, T); \tag{13}$$

$$dp = \left(\frac{\partial p}{\partial T}\right)_{\Delta f} dT + \left(\frac{\partial p}{\partial \Delta f}\right)_{T} d\Delta \tag{14}$$

From (8),

$$\left(\frac{\partial p}{\partial T}\right)_{\Delta f} = -\frac{\Delta f \cdot p(1-p)}{kT^2} \tag{15}$$

$$\left(\frac{\partial p}{\partial \Delta f}\right)_{T} = -\frac{p(1-p)}{kT} \tag{16}$$

Therefore, substituting (15) and (16) in (14);

$$\frac{dp}{dT} = -\frac{p(1-p)}{kT} \cdot \left(\frac{\Delta f}{T} + \frac{d\Delta f}{dT}\right) \tag{17}$$

and from (10),

$$\frac{dp}{dT} = -\frac{p(1-p)}{kT} \cdot \left(\frac{\Delta f}{T} + s\right). \tag{18}$$

The left hand side of (18) plotted against temperature is the curve (Fig. 11) giving the amount of α-phase formed per unit temperature change. The number of units transforming to α at 420° K is small; at 421 it is considerably larger. At T_m(423° K) the number of units transforming is greater than at any other temperature. At temperatures above T_m the number of units transforming is smaller and smaller. The curve is a normal distribution curve. Equation 18 was derived by differentiation of the empirical equations for the observed curves (Fig. 8). These observed curves obtained by TDA are therefore representations of the integral of

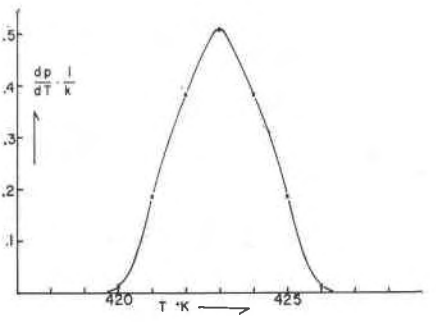

FIG. 11. dp/dT *vs.* T for transformation with rising temperature; a normal distribution curve.

Equation 18 showing the fraction of the transformation complete at a given temperature or the cumulative sum of the area under the curve of Fig. 11. In both cases, the value of the ordinate is independent of the time taken to reach the temperature and independent of the time held at the temperature. Such time-independent processes indicate the absence of diffusion from the mechanism of transformation. The conclusions, however, might not apply over geological time.

HYSTERESIS

Although the runs for Fig. 7 establish the diffusionless character of the transformation and, therefore, the essential time-independence of the p *vs.* T curves (Fig. 8), there is ample evidence of mobility of the AgI units of structure. The high mobility of the Ag ions is treated by Lieser (1957). We wish to account for the failure of a transformation, once initiated, to proceed isothermally to completion. Apparently, two phases coexist in thermal equilibrium over a band of temperatures and not simply at a single critical temperature of transformation. We account for this by assuming that the free energies of the phases involved are to be represented by curves such as those of Fig. 12. Because of the positive curvature of the dependence of the free energies on T, there is a range of temperature around T_m within which mixtures of the two phases have a lower total energy than either of the two phases. The free energy of the transforming system is represented by the line tangent to the free energy curves of the two phases. A point on the line represents the minimum free energy of the system at that temperature; this minimum free energy is reached by the proportions of the two phases given by the lever law. As there are two transformation temperatures, T_m^{H-L} and T_m^{L-H}, there must be two sets of curves such as Figure 12 and it is this doubling of the curves of Figure 12 which comprises the hysteresis.

Simultaneous, continuous records of p *vs.* T and p *vs.* t (time) were obtained with both showing the s or ƨ character. The transformation

begins with a slow nucleation involving the formation of isolated domains of the new phase. But the transformation may proceed largely by the migration of the domain walls, that is, major changes in p may be accompanied by only slight increase in the amount of domain wall separating the two phases. In the vicinity of T_m, and beyond T_m while the transformation proceeds from p(0.5) to completion, the amount of domain wall

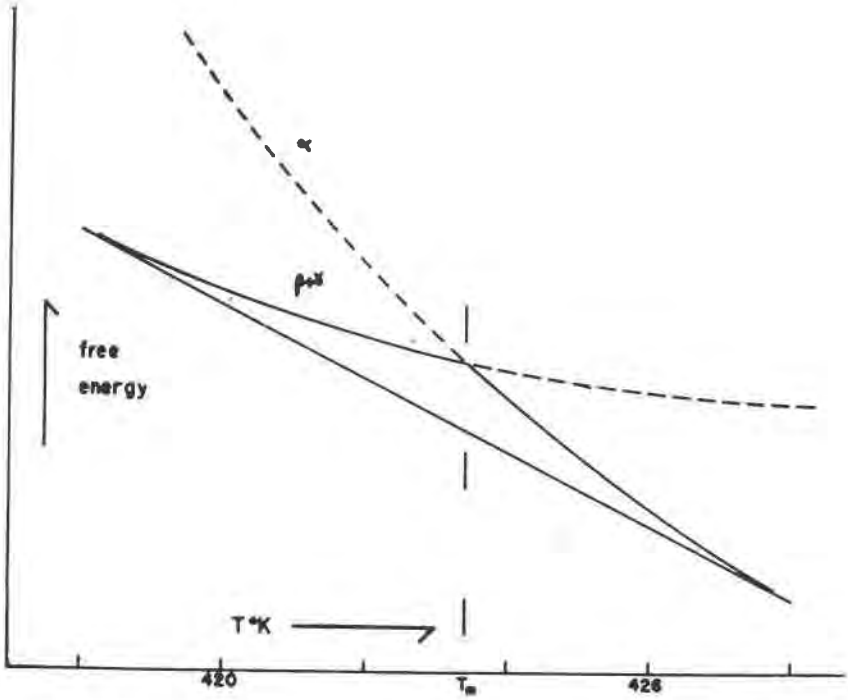

FIG. 12. Hypothetical free energy *vs.* T curves for transformation with rising temperature. Although the free energy *vs.* T curves for the low and high temperature phases intersect at T_m, mixtures of the low and high phases have total free energies represented by the straight line tangent to the curves and lower than either. The phase proportions at any point on the line are given by the lever law.

actually decreases with return of activation energy. By analogy with ferromagnetic domains, one imagines peculiarly oriented grains or defective crystallites being particularly resistant to the transformation, accounting for the last final tapering off of the s-curves. Although the transformation is produced entirely by the flow of heat, the physical changes involved in the initiation and migration of the domain walls are in effect, work.

From the loop of Fig. 8a, it is possible to conceive of a heat engine

operating in a cycle. If the s-curves are straightened out, they become two isothermal steps connected by two symmetric anisothermal steps. We imagine the specimen in the shape of a cylinder undergoing a cyclic contraction and expansion along the axis, and connected by a suitable eccentric to a pump rod or other working device.

In the high temperature step, heat flows into the crystal, the crystal contracts, the pump rods are raised against the force of gravity. In the low temperature step, heat flows out of the crystal, the crystal expands, the pump rods fall. In the absence of hysteresis the process may repeat indefinitely. But if there are to be any losses, any internal friction or external work—if for example, water is to be raised with the power stroke of the pump rod and not dropped again, the heat flow to the crystal in the L-H step must be greater than the heat flow from the crystal in the H-L step, by the amount of work done plus the frictional losses. In our experiments, no work is performed, the force against which the crystal changes volume is that of one atmosphere—essentially negligible. The hysteresis is due solely to internal friction. As the domain walls move across the sample, warping bond angles and crossing grain boundaries, energy beyond that of the latent heat is required. This frictional work W is manifest in a greater heat flow which in turn is possible at a higher temperature. In a complete cycle, frictional work of 2W is performed. In the cycle, heat is absorbed in the transformation at 423° and a smaller amount of heat is rejected in the transformation back at 411°. At the end of the cycle, the universe is unchanged except for this flow of heat.

In the absence of internal friction the heat rejected would exactly equal the heat accepted and the complete cycle would occur at one temperature. The transformation would be a reversible process. Considering the possibilities of mechanical linkage, given a reversible transformation with a dimensional change, heat could be continuously converted to work with no other changes. It therefore appears that no phase transformation involving a dimensional change may occur completely reversibly or, *all phase transformations involving dimensional changes against finite resistance exhibit hysteresis*. From the figures for s in equations 12 for the loop of Fig. 8a, a total hysteresis loss of $\Delta s \cdot \Delta T$ or 300 cal/mol is obtained. This figure should be reduced by allowing for the difference in specific heats in the two anisothermal steps; a correction of the order of 50 cal/mol; numbers which should be taken with the degree of skepticism reserved for non-calorimetric values.

Conclusions

The procedures which we have lumped together under the term *thermal diffraction analysis* facilitate a detailed examination of the process of phase transformation. We believe that our results establish the existence

of a type of heterogeneous phase transformation characterized by the s or ƨ-shape of the TDA curve, and by a thermal hysteresis. These effects are interpreted as the result of the lowering of the total free energy of mixtures of two phases and of the appearance of a two-dimensional intermediate phase—the domain walls—requiring high activation energy Q. Because the migration of the domain walls in the transformation is mechanical work and because no process involving the conversion of heat to work can be completely reversible, there is a thermal hysteresis for the transformation, the hysteresis loss being given by the area of the loop. Any proportion of high and low phases are stable (for practical purposes) at any temperature within the loop. The transformation is essentially diffusionless.

The β to γ transformation does not proceed appreciably at constant temperature. No sign of the reported critical temperature for the transformation between 125 and 135° C. is observed in dynamic or static runs but mechanical working with falling temperatures yields samples with powder diffraction patterns for 97% cubic material, from initially pure hexagonal material. The transformation β to γ is also diffusionless and here classed as martensitic. An apparent influence of the D- or γ-ratio on the width of the hysteresis loop is believed evidence for the existence of a variable order parameter in the high temperature phase.

No evidence of polytypism appeared in these experiments. On theoretical grounds (Schneer, 1955) the γ-ratio (D) is a function of temperature but in the absence of isothermal transformation, the evaluation of D as a function of T was not obtained. But samples transform from α to a $\gamma+\beta$ mixture D(0.40) at about 138° C. and if this is taken as the equilibrium γ-ratio at 138° C., it indicates that the critical temperature for the γ to β transformation where D falls to 0, is at still higher temperatures, unobtainable because of the intervention of the high temperature α transformation.

The phenomenon of hysteresis illustrates a general principle of indeterminism in geological science. A fixed configuration of phases is not uniquely prescribed by the thermodynamic coordinates but may instead have been reached by an indefinitely large number of pathways. Similarly there is not one past history to the present configuration of the earth but an infinity of histories. The geologic past is not a part of nature uniquely prescribed by the records of the present but must remain a part of science —a free construction of mind in nature.

Acknowledgments

This work was accomplished under the auspices of grants from the National Science Foundation, the Frederick Gardiner Cottrell fund of the

Research Corporation, the Graduate School of the University of New Hampshire and the M.I.T. Computation Center. Roy Vezina, Harry Gladwin and Jean Sansbury assisted in the measurements. We trace many of these ideas to discussion with Professors John Mulhern, Lyman Mower and Sidney Butler, of the U.N.H. Department of Physics, Professor Robert Garrels of the Harvard Department of Geology and Dr. W. Baltensperger of the Physics Institute of the Swiss Federal Institute of Technology. We have compared notes with Professor Clark Stephenson and Mr. David Waldbaum (1960) of the M.I.T. Department of Chemistry. None of the above agencies or individuals have in any way approved or disapproved any of the statements which may appear above, but for their combined generosity and intelligence, we wish to make grateful acknowledgement.

Appendix I

TDA records were obtained using the furnace for diffractometer manufactured by Tem-Pres. Inc., State College, Pennsylvania, mounted on the G.E. XRD 5. The amplifier for the vertical circuit of a Houston HR-92 X-Y recorder was connected in parallel with the amplifier of the diffractometer recorder. The calibration controls of the X-Y recorder were adjusted to bring the Y-axis amplification to match the diffractometer recorder. The thermocouple in contact with the sample (actually in contact with the Pt-Rh sample holder) was connected through a separate pre-amplifier (Houston M10-F) to the X-axis amplifier of the recorder. In order to restrict attention to the significant temperature range (and to spread the hysteresis loop over the chart) a bucking voltage was introduced (see schematic diagram, Fig. 13). Calibration was by means of a potentiometer.

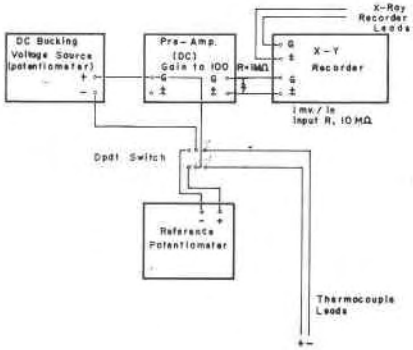

FIG. 13. Schematic diagram of the assembly for the TDA records of Figs. 8a and 8b. The reference potentiometer is used as a source of variable D. C. to calibrate the X-Y recorder. It may also be connected in parallel with the thermocouple for exact measurements during the run, (dotted lines).

Appendix II

Preparation of physically pure AgI; A. β-phase.

To 30 grams of reagent grade AgI in a 4L beaker add approximately 700 ml distilled water. Add reagent grade KI until with stirring, all AgI is dissolved (up to 300 grams). Precipitate by adding distilled water at a rate of approximately 80 drops per minute until drops falling on the solution produce no further precipitation or cloudiness on contact. Decant after settling, wash with distilled water. Repeat until wash water tested with $AgNO_3$

fails to produce cloudy precipitate of AgI. Blot off excess water with filter paper and dry in a desiccator at room temperature. Avoid any shearing pressures.

B. γ-phase is prepared from chemically pure AgI (β-phase prepared as above) by repeated grinding while the temperature falls from the boiling point to that of the room. A mortar is mounted above a pan of boiling water and grinding continued until the water is no longer hot. Two or three cycles produce material yielding diffraction patterns 95%+γ.

References

Bloch, R. and H. Möller (1931) Ueber die Modifikationen des Jodsilbers, *Zeit. physik. Chem.* **152,** 245–268.

Becker, R. (1938) Nuclear formation in the separation of metallic mixed crystals. *Ann. Phys.* **32,** 128.

Cullity, B. D. (1956) *Elements of X-ray Diffraction*, Addison-Wesley, Reading, Mass.

Ewald, P. P. and C. Hermann (1931) *Strukturberichte*, **I,** 1913–1926.

Gottfried, C. and F. Schossberger (1937) *Strukturberichte*, **III,** 1933–1935.

Greninger, A. B. (1939) The martensite transformation in beta copper-aluminum alloys. *Trans. A.I.M.E.* **133,** 204–227.

Herrmann, K. (1941) *Strukturberichte*, **VI,** 1938.

Kaufman, L. and M. Cohen (1958) Thermodynamics and kinetics of martensitic transformations, *Prog. Met. Physics*, **7,** 165.

Kelley, K. K. (1949) Contributions to the data on theoretical metallurgy—X; High-temperature heat-content, heat capacity, and entropy data for inorganic compounds, *U. S. Bureau Mines Bull.* **476,** 160.

Lieser, K. H. (1957) Fehlordnungserscheinungen und Umwandlungsvorgänge im Silberjodid, *Forts. Min.* **36,** (2), 96–118.

Pitzer, K. S. (1941) Heat capacity and entropy of AgI and their interpretation in terms of structure. *Jour. Am. Chem. Soc.* **63,** 516–518.

Schneer, C. J. (1955) Polymorphism in one-dimension, *Acta Cryst.* **8,** 279.

Strock, L. W. (1956) Erganzung und Berichtigung zu Kristallstruktur des Hochtemperatur—Jodsilbers—AgI, *Zeit. physik. Chem.* **B31,** 132.

Swanson, H. E., N. T. Gilfrich, M. I. Cook, R. Stinchfield and P. C. Parks (1959) Standard x-ray diffraction powder patterns. *N.B.S. Circ.* **539, 8,** 52.

Wahl, F. M., R. E. Grim and R. B. Graf (1961) Phase transformations in silica as examined by continuous x-ray diffraction. *Am. Mineral.* **46,** 196–208.

Waldbaum, D. R. (1960) Structural and Thermodynamic Properties of Silver Iodide. M.S. Thesis, Dept. Geol. and Geophysics, M.I.T.

Manuscript received, August 3, 1962; accepted for publication, April 9, 1963.